を明らかにすることもできた。一方、このような収量の低い株は、培養条件を変えることで、ある程度の収量改善の可能性があることを示した。また、永田研究代表との共同研究にて、各候補ウイルス株の HA による細胞侵入過程以外の細胞内での転写・複製など増殖効率に関しても、ウイルスに必要とされる宿主因子との関連性を含め、解析を展開しているところである。

F. 健康危険情報

なし

G. 研究発表

1. 論文発表

1) Shirakura M, Kawaguchi A, Tashiro M, Nobusawa E. Composition of Hemagglutinin and Neuraminidase Affects the Antigen Yield of Influenza A (H1N1)pdm09 Candidate Vaccine Viruses. Jpn. J. Infect. Dis., 2013; 66(1): 65-68.
2) Uchida Y, Suzuki Y, Shirakura M, Kawaguchi A, Nobusawa E, Tanikawa T, Hikono H, Takemae N, Mase M, Kanehira K, Hayashi T, Tagwa Y, Tashiro M, Saito T. Genetics and infectivity of H5N1 highly pathogenic avian influenza viruses isolated from chickens and wild birds in Japan during 2010-2011. Virus Res., 2012; 170: 109-117.

2. 学会発表

1) 信澤枝里、中内美名、松嵜葉子、菅原勘悦、有田知子、廣津伸夫、田代眞人、西村秀一. A/H1N1pdm09 ワクチン被接種者血清抗体が認識する HA 上の抗原領域の解析. 第 60 回日本ウイルス学会学術集会. 大阪： 2012 年 11 月
2) 松嵜葉子、菅原勘悦、下平義隆、本郷誠治、信澤枝里. パンデミックインフルエンザ A/H1N1pdm09 の HA 分子の抗原構造の解析. 第 60 回日本ウイルス学会学術集会. 大阪： 2012 年 11 月
3) 嶋崎典子、白倉雅之、信澤枝里、矢野茂生、板村繁之、田代眞人. インフルエンザワクチン製造株のアミノ酸変異による抗原蛋白経時安定性への影響. 第 60 回日本ウイルス学会学術集会. 大阪： 2012 年 11 月
4) 川口晶、鈴木忠樹、相内章、佐藤由子、信澤枝里、田代眞人、長谷川秀樹. 喘息発作誘発モデルを用いたインフルエンザウイルス感染症の病態解析. 第 60 回日本ウイルス学会学術集会. 大阪：2012 年 11 月
5) 有田知子、白倉雅之、信澤枝里、田代眞人. H5N1 インフルエンザワクチン種株候補の抗原収量の検討. 第 16 回日本ワクチン学会学術集会. 横浜：2012 年 11 月

H. 知的財産権の出願・登録状況（予定を含む。）

1．特許出願

なし

2．実用新案登録

なし

3．その他

なし

II. 研究成果の刊行に関する一覧表

発表者氏名	論文タイトル名	発表誌名	巻号	ページ	出版年
Haruyama T, Nagata K.	Anti-influenza virus activity of Ginkgo biloba leaf extracts.	J. Nat. Med.	—	in press	2012
Onomoto K, Jogi M, Yoo JS, Narita R, Morimoto S, Takemura A, Sambhara S, Kawaguchi A, Osari S, Nagata K, Matsumiya T, Namiki H, Yoneyama M, Fujita T.	Critical role of antiviral stress granule containing RIG-I and PKR in viral detection and innate immunity.	PLoS One	7(8)	e43031	2012
Kawamura M, Kusano A, Furuya A, Hanai N, Tanigaki H, Tomita A, Horiguchi A, Nagata K, Itazawa T, Adachi Y, Okabe Y, Miyawaki T, Kohno H.	New sandwich-type enzyme-linked immunosorbent assay for human MxA protein in a whole blood using monoclonal antibodies against GTP-binding domain for recognition of viral infection.	J. Clin. Lab. Anal.	26(3)	174-183	2012
Kawaguchi A, Matsumoto K, Nagata K.	YB-1 functions as a porter to lead influenza virus ribonucleoprotein complexes to microtubules.	J. Virol.	86(20)	11086-11095	2012
Komatsu T, Nagata K.	Replication-uncoupled histone deposition during adenovirus DNA replication.	J. Virol.	86(12)	6701-6711	2012
Kato SI, Nagata K, Takeuchi K.	Cell tropism and pathogenesis of measles virus in monkeys.	Front. Microbiol.	3	14	2012
Okuwaki M, Sumi A, Hisaoka M, Saotome-Nakamura A, Akashi S, Nishimura Y, Nagata K.	Function of homo- and hetero-oligomers of human nucleoplasmin/nucleophosmin family proteins NPM1, NPM2 and NPM3 during sperm chromatin remodeling.	Nucleic Acids Res.,	40(11)	4861-4878.	2012
Samad MA, Komatsu T, Okuwaki M, Nagata K.	B23/nucleophosmin is involved in regulation of adenovirus chromatin structure at late infection stages, but not in virus replication and transcription.	J. Gen. Virol.	93(6).	1328-1338	2012

Czene A, Nemeth E, Zoka IG, Jakab-Simon N, Kortvelyesi T, Nagata K, Christensen HEM, Gyurcsik B.	The role of the N-terminal loop in the function of the colicin E7 nuclease domain.	J. Biol. Inorg. Chem.	18(3)	309-321	2013
Nishiyama T, Noguchi H, Yoshida H, Park SY, Tame JR.	The structure of the deacetylase domain of Escherichia coli PgaB, ad enzyme required for biofilm formation: a circularly permuted member of the carbohydrate esterase 4 family.	Acta. Crystallogr. D. Biol. Crystallogr.	69(1)	44-51	2013
Noguchi H, Campbell KL, Ho C, Unzai S, Park SY, Tame JR.	Structure of haemoglobin from woolly mammoth in liganded and unliganded states.	Acta. Crystallogr. D. Biol. Crystallogr.	68(11)	1441-1449	2012
Yoshida H, Kawai F, Obayashi E, Akashi S, Roper DI, Tame JR, Park SY.	Crystal structures of penicillin-binding protein 3 (PBP3) from methicillin-resistant Staphylococcus aureus in the apo and cefotaxime-bound forms.	J. Mol. Biol.	423(3)	351-364	2012
Hansman GS, Taylor DW, McLellan JS, Smith TJ, Georgiev I, Tame JR, Park SY, Yamazaki M, Gondaira F, Miki M, Katayama K, Murata K, Kwong PD.	Structural basis for broad detection of genogroup II norobiruses by a monoclonal antibody that binds to a site occluded in the viral particle.	J. Virol.	86(7)	3635-3646	2012
Murakami K, Ichinohe Y, Koike M, Sasaoka N, Iemura S, Natsume T, Kakizuka A.	VCP is an integral component of a novel feedback mechanism that controls intracellular localization of catalase and H_2O_2 levels.	PLoS One	8(2)	e56012	2013
Sekine Y, Hatanaka R, Watanabe T, Sono N, Iemura SI, Natsume T, Kuranaga E, Miura M, Takeda K, Ichijo H.	The kelch repeat protein KLHDC10 regulates oxidative stress-induced ASK1 activation by suppressing PP5.	Mol. Cell	48(5).	692-704	2012
Okatsu K, Iemura S, Koyano F, Go E, Kimura M, Natsume T, Tanaka K, Matsuda N.	Mitochondrial hexokinase HKI is a novel substrate of the Parkin ubiquitin ligase.	Biochem. Biophys. Res. Commun.	428(1)	197-202.	2012

Fujimoto M, Takaki E, Takii R, Tan K, Prakasam R, Hayashida N, Iemura S, Natsume T, Nakai A.	RPA assists HSF1 access to nucleosomal DNA by recruiting histone chaperone FACT.	Mol. Cell	48(2)	182-194	2012
Ishfaq M, Maeta K, Maeda S, Natsume T, Ito A, Yoshida M.	Acetylation regulates subcellular localization of eukaryoic translation initiation factor 5A (eIF5A).	FEBS Lett.,	586(19)	3236-3241	2012
Yoshihara H, Fukushima T, Hakuno F, Saeki Y, Tanaka K, Ito A, Yoshida A, Iemura S, Natsume T, Asano T, Chida K, Girnita L, Takahashi S.	Insulin/insulin-like growth factor (IGF) stimulation abrogates an association between a deubiquitinating enzyme USP7 and insulin receptor substrates (IRSs) followed by proteasomal degradation of IRSs.	Biochem. Biophys. Res. Commun.	423(1)	122-127	2012
Matsushita K, Kajiwara T, Tamura M, Satoh M, Tanaka N, Tomonaga T, Matsubara H, Shimada H, Yoshimoto R, Ito A, Kubo S, Natsume T, Levens D, Yoshida M, Nomura F.	SAP155-mediated splicing of FUSE-binding protein-interacting repressor serves as a molecular switch for c-myc gene expression.	Mol. Cancer Res.	10(6)	787-799	2012
Kobayashi H, Harada H, Nakamura M, Futamura Y, Ito A, Yoshida M, Iemura S, Shin-ya K, Doi T, Takahashi T, Natsume T, Imoto M, Sakakibara Y.	Comprehensive predictions of target proteins based on protein-chemical interaction using virtual screening and experimental verifications.	BMC Chem. Biol.	12(1)	2	2012
Ideue T, Adachi S, Naganuma T, Tanigawa A, Natsume T, Hirose T.	U7 small nuclear ribonulceoprotein represses histone gene transcription in cell cycle-arrested cells.	Proc. Natl. Acad. Sci. USA	109(15)	5693-5698	2012
Abe J, Nagai Y, Higashikuni R, Iida K, Hirokawa T, Nagai H, Kominato K, Tsuchida T, Hirata M, Inada M, Miyaura C, Nagasawa K.	Synthesis of vitamin D3 derivatives wih nitrogen-linked substituents at A-ring C-2 and evaluation of their vitamin D receptor-mediated transcriptional activity.	Org. Biomol. Chem.	10(38)	7826-7839	2012

Shirakura M, Kawaguchi A, Tashiro M, Nobusawa E.	Composition of Hemagglutinin and Neuraminidase Affects the Antigen Yield of Influenza A (H1N1)pdm09 Candidate Vaccine Viruses.	Jpn. J. Infect. Dis.	66(1)	65-68.	2013
Uchida Y, Suzuki Y, Shirakura M, Kawaguchi A, Nobusawa E, Tanikawa T, Hikono H, Takemae N, Mase M, Kanehira K, Hayashi T, Tagwa Y, Tashiro M, Saito T.	Genetics and infectivity of H5N1 highly pathogenic avian influenza viruses isolated from chickens and wild birds in Japan during 2010-2011.	Virus Res.	170	109-117.	2012

III. 研究成果の刊行物・別刷

J Nat Med
DOI 10.1007/s11418-012-0725-0

ORIGINAL PAPER

Anti-influenza virus activity of *Ginkgo biloba* leaf extracts

Takahiro Haruyama · Kyosuke Nagata

Received: 27 July 2012 / Accepted: 9 November 2012

Abstract We examined the influence of *Ginkgo biloba* leaf extract (EGb) on the infectivity of influenza viruses in Madin–Darby canine kidney (MDCK) cells. Plaque assays demonstrated that multiplication of influenza viruses after adsorption to host cells was not affected in the agarose overlay containing EGb. However, when the viruses were treated with EGb before exposure to cells, their infectivity was markedly reduced. In contrast, the inhibitory effect was not observed when MDCK cells were treated with EGb before infection with influenza viruses. Hemagglutination inhibition assays revealed that EGb interferes with the interaction between influenza viruses and erythrocytes. The inhibitory effect of EGb was observed against influenza A (H1N1 and H3N2) and influenza B viruses. These results suggest that EGb contains an anti-influenza virus substance(s) that directly affects influenza virus particles and disrupts the function of hemagglutinin in adsorption to host cells. In addition to the finding of the anti-influenza virus activity of EGb, our results demonstrated interesting and important insights into the screening system for anti-influenza virus activity. In general, the plaque assay using drug-containing agarose overlays is one of the most reliable methods for detection of antiviral activity. However, our results showed that EGb had no effects either on the number of plaques or on their sizes in the plaque assay. These findings suggest the existence of inhibitory activities against the influenza virus that were overlooked in past studies.

Keywords Antiviral effect · *Ginkgo biloba* leaf extract · Hemagglutination · Influenza virus

T. Haruyama · K. Nagata (✉)
Department of Infection Biology, Faculty of Medicine and Graduate School of Comprehensive Human Sciences, University of Tsukuba, 1-1-1 Tennodai, Tsukuba 305-8575, Japan
e-mail: knagata@md.tsukuba.ac.jp

Present Address:
T. Haruyama
Research Center, AVSS Corporation, 1-22 Wakaba-machi, Nagasaki 852-8137, Japan

Introduction

Influenza viruses, members of the *Orthomyxoviridae* family, cause epidemics in the human population every year despite the availability of effective vaccines. In a severe pandemic year, millions of people die from the infection. Influenza viruses are classified on the basis of the antigenic properties of two surface glycoproteins: hemagglutinin (HA) and neuraminidase (NA). Sixteen HA subtypes (H1–H16) and nine NA subtypes (N1–N9) have so far been defined. Influenza virus infection is initiated by the interaction between HA and sialic acid moieties of glycoconjugates on host cells [16].

Several synthetic drugs such as amantadine and rimantadine (M2 ion channel inhibitors) and oseltamivir and zanamivir (NA inhibitors) have been available for decades, but all have side effects and thus somewhat limited usefulness [6, 11]. Therefore, novel substances and approaches are needed to control and prevent this viral disease. Various natural products have distinct anti-influenza virus activities [14]. We have demonstrated that a high-molecular-weight lignin-related fraction extracted from cones of *Pinus parviflora* Siebold et Zucc. suppresses the multiplication of influenza viruses by preventing viral RNA synthesis [9, 15]. We also reported that *Sanicula europaea* L. leaf extract contains an anti-influenza virus substance(s) that selectively inhibits influenza A viruses, but

Published online: 22 November 2012

not influenza B viruses [13]. Studies on the anti-influenza virus activity of natural products have dramatically increased over the past several years [14].

Ginkgo biloba leaf extract (EGb) is a potential phytomedicine with various pharmacologic effects: in particular, anticoagulant, vasodilator, and anti-inflammatory effects [17]. In many countries, EGb and similar products are prescribed as therapeutic agents for cerebral or peripheral vascular inefficiency and for cognitive impairments associated with aging [2, 3]. Unlike other herbal drugs, however, EGb has hardly been tested for its anti-influenza virus activity. In the present study, we examined the inhibitory effect of EGb on influenza viruses.

Materials and methods

Reagents

The powder of *Ginkgo biloba* leaf extract was prepared by Mitsubishi Paper Mills Co., Ltd., Japan. In brief, the dried *Ginkgo biloba* leaves were finely ground and then extracted with water containing alcohol. After removing the residue, the extracts were concentrated under reduced pressure. The concentrate was then filtered and treated with adsorption resin to eliminate the impurities. Finally, the extracts were concentrated under reduced pressure again and then dried to use as powder. The powder of *Ginkgo biloba* leaf extract was dissolved in DMSO at a concentration of 100 mg/ml and stored at −30 °C until use.

As main active ingredients, it is known that the extract contains not only flavonoids such as kaempferol, quercetin and isorhamnetin but also terpene lactones such as bilobalide, ginkgolide A, B, C and J as specific components derived from *Ginkgo biloba* leaves [1, 4, 5].

Cells and viruses

Madin–Darby canine kidney (MDCK) cells were maintained in Eagle's minimum essential medium (MEM) at 37 °C, in a 5 % CO_2 atmosphere, supplemented with 10 % fetal bovine serum, 0.03 % L-glutamine, 100 U/ml penicillin and 100 μg/ml streptomycin.

Influenza A/PR/8/34 (H1N1), A/Udorn/72 (H3N2), and B/Lee/40 viruses were grown at 35.5 °C for 48 h in allantoic sacs of 11-day-old embryonated eggs (Miyake Hatchery), and then the infected allantoic fluid was collected and stored at −80 °C until use.

Neutral red assay

The neutral red assay is based on incorporation of neutral red into lysosomes in living cells. To determine the effect of EGb on cell viability, MDCK cells (3.5×10^4 cells/well) were seeded into 24-well tissue culture plates and kept at 37 °C overnight. After removal of the culture medium, 0.4 ml of MEM containing various concentrations of EGb or DMSO was added to each well of the plates. After incubation for 24 h at 37 °C, 0.2 ml of neutral red solution (0.15 mg/ml) was added to each well. After incubation at 37 °C for 3 h, wells were washed with 0.2 ml of a fixative (1 % formalin and 1 % $CaCl_2$). To extract the dye, 0.2 ml of 1 % acetic acid in 50 % ethanol was added to each well. After incubation at room temperature for 20 min, the amount of neutral red in each well was determined by measuring absorbance at 550 nm using a spectrometer. Results were represented as the cell number that was calculated from the standard curve of cell numbers. Furthermore, to determine the effect of EGb on the cell growth, MDCK cells (2.0×10^4 cells/well) were seeded into 24-well tissue culture plates and kept at 37 °C overnight. After removal of the medium, 0.4 ml of MEM containing 0, 10 and 100 μg/ml of EGb were added to each well. As control groups, DMSO was added to each well at final concentrations of 0.01 or 0.1 %. After incubation at 37 °C for 0, 24, 48 and 72 h, viable cells were determined with the neutral red assay as described above.

Treatment of viruses and cells by EGb

For pre-treatment of viruses by EGb, influenza A/PR/8/34 virus (500 pfu/ml) was mixed with EGb at several concentrations, incubated at room temperature for 10 min, and then subjected to the plaque formation assay. For post-treatment by EGb, MDCK cells infected with influenza viruses were overlaid with 0.8 % agarose containing EGb at several concentrations in the plaque formation assay. To investigate the direct effect of EGb on host cells, MDCK cells were exposed to EGb at several concentrations and incubated at 37 °C for 1 h. After removing the medium containing EGb, MDCK cells were infected with influenza viruses followed by the plaque formation assay.

Plaque formation assay

A confluent monolayer culture of MDCK cells in a 6-well tissue culture plates was washed with serum-free MEM and then infected with 0.5 ml of influenza virus solution [500 pfu/ml = multiplicity of infection (MOI) of 2.5×10^{-4}] in serum-free MEM. After allowing 1 h at 37 °C for virus adsorption, the cells were washed with serum-free MEM and then overlaid with MEM containing 0.8 % agarose, 0.2 % BSA and 1 μg/ml L-1-tosylamide-2-phenylethyl chloromethyl ketone (TPCK)-treated trypsin (Sigma). After incubation at 37 °C for 2–3 days, plaques were visualized by staining cells with 0.5 % amido black.

Results were represented as a ratio of the plaque number formed in the presence of EGb to that in the absence of EGb.

Hemagglutination assay

Influenza A/PR/8/34 virus (2×10^8 pfu/ml) was diluted nine times with phosphate buffered saline (PBS) (−) by twofold dilution each time, while 200 μg/ml of EGb was also diluted ten times with PBS (−) containing 0.2 % DMSO by twofold dilution each time. Fifty microliters of each diluted virus was mixed with 50 μl of each diluted EGb. These mixtures were then maintained at room temperature for 5 min. One hundred microliters of 0.5 % chicken erythrocyte suspension (Nippon Bio-Test Laboratories Inc., Japan) was added to each of these mixtures in 96-well round-bottom plates, and then the plate was incubated at room temperature for 30 min for hemagglutination. Results were represented as a plot where the *x*-axis and *y*-axis indicate concentrations of EGb and HA titer, respectively.

Statistical analysis

All of the data were represented as mean ± standard error of the mean (SEM). Comparisons for all pairs were performed by Student's *t* test. A *p* value >0.05 was considered to be not significant. The calculations of 50 % cytotoxicity concentration (CC_{50}) and inhibitory concentrations with 50 % plaque reduction (IC_{50}) were performed by nonlinear regression using GraphPad Prism's "log (inhibitor) versus response − variable slope" function (GraphPad Prism Version 5.01 for Windows, GraphPad Software Inc.).

Results

Effect of EGb on the viability and growth of MDCK cells

Before examining the anti-influenza virus activity of EGb, we investigated whether EGb affects the viability and growth of MDCK cells, which are routinely used as host cells for influenza viruses. We evaluated the cell viability and growth by counting the number of living cells as a function of time using the neutral red assay as described in "Materials and methods". Cytotoxic effects of EGb were not observed at concentrations of <10 μg/ml (CC_{50} = 180 μg/ml) (Fig. 1a). Neither the growth rate nor the final cell density was affected by the presence of 10 μg/ml of EGb, whereas a marked decrease in the cell growth rate was observed at 100 μg/ml (Fig. 1b). Thus, EGb at a concentration of <10 μg/ml could be considered essentially nontoxic to MDCK cells. We confirmed that the solvent DMSO had no effect on the viability and growth of MDCK cells in the range of concentrations used in this study (data not shown).

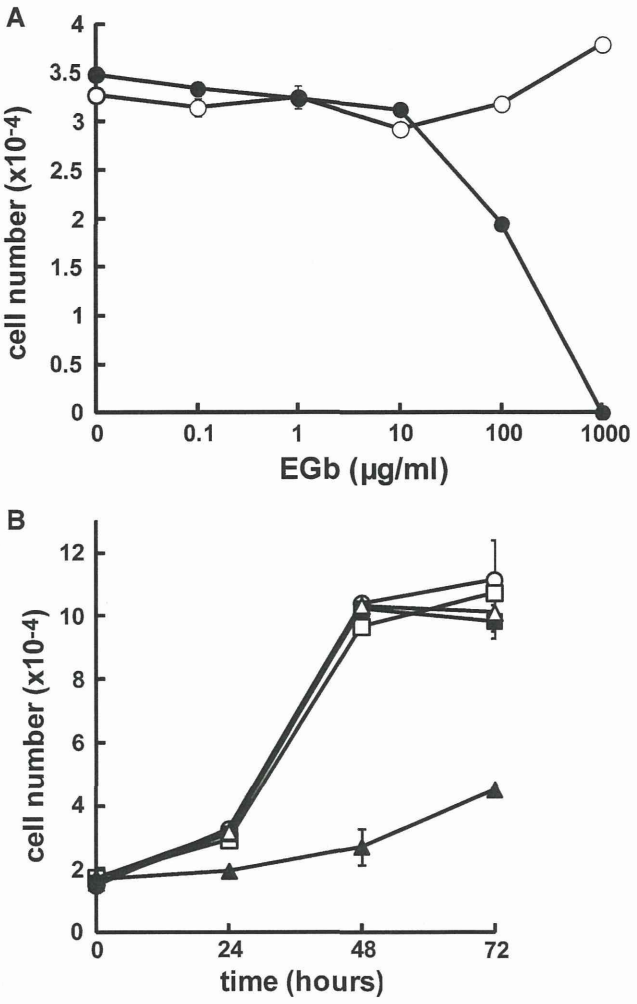

Fig. 1 Effect of EGb on the viability and the growth of MDCK cells. **a** MDCK cells (3.5×10^4) were seeded in 24-well tissue culture plates and incubated at 37 °C in the presence of various concentrations of EGb (*closed circles*) or solvent DMSO alone (*open circles*). After incubation for 24 h, the viable cell number was determined by the neutral red assay. **b** MDCK cells (2×10^4) were seeded in 24-well tissue culture plates and incubated at 37 °C in the absence (*open circles*) or presence of 10 μg/ml (*closed square*) and 100 μg/ml (*closed triangles*) of EGb, and 0.01 % (v/v) and 0.1 % (v/v) of DMSO alone (*open square* and *open triangle*, respectively). After incubation for the indicated periods, the viable cell number was determined by the neutral red assay

Inhibition of influenza virus infectivity by EGb

To examine whether EGb inhibits multiplication of influenza viruses, plaque assays were carried out as described in "Materials and methods". Cells were infected with influenza A/PR/8/34 virus at 37 °C for 1 h. The cells were

washed extensively with serum-free MEM and then overlaid with 0.8 % agarose in MEM containing EGb at various concentrations. The number of plaques and their sizes in the presence of EGb did not differ from those in the absence of EGb (Fig. 2a), indicating that EGb does not inhibit plaque formation by influenza virus infection. We further examined whether EGb is effective when mixed with viruses before exposure to cells. Influenza viruses were mixed with EGb at various concentrations at room temperature for 10 min and then exposed to MDCK cells. Under these conditions, EGb markedly inhibited viral infectivity in a dose-dependent manner (Fig. 2b). EGb at a concentration of 5 μg/ml almost completely inhibited the plaque-forming activity. These findings suggest that EGb inhibits the initial step of influenza virus infection before the virus enters the cytoplasm. Next, we examined whether the inhibitory effect of EGb against influenza virus was direct or indirect. Plaque assays were performed using MDCK cells treated with EGb at various concentrations for 1 h before infection with the influenza viruses. The number and sizes of the plaques of the tested groups in the presence of EGb did not differ significantly from those of the control group in the absence of EGb (Fig. 3), suggesting that EGb directly interacted with the influenza viruses and markedly reduced their infectivity.

Inhibition of hemagglutination by EGb

Influenza virus infection is initiated by the interaction of hemagglutinin (HA) on the virion with sialic acids on the host cell surface. To understand how EGb prevents virus adsorption to cells, we examined whether EGb competitively inhibits influenza virus-mediated hemagglutination. As shown in Fig. 4, EGb inhibited hemagglutination in a dose-dependent manner, suggesting that EGb interferes with the interaction between HA and sialic acids.

Susceptibility of other influenza virus strains to EGb

Our results suggest that EGb binds to HA and prevents virus adsorption to cells. We further examined whether the inhibitory effect of EGb is dependent on the type of influenza virus. EGb inhibited the infectivity of both influenza A/Udorn/72 (H3N2) and influenza B/Lee/40 viruses as well as of influenza A/PR/8/34 (H1N1) virus in an adsorption inhibition-dependent manner (compare Fig. 5a and b), albeit

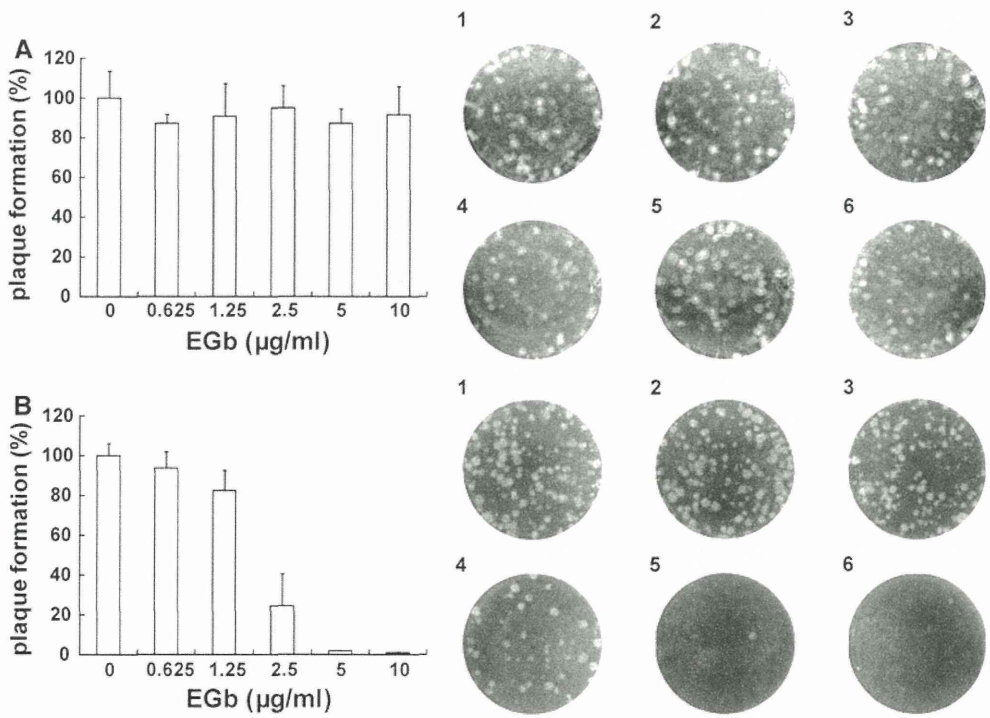

Fig. 2 Effect of EGb on plaque formation. Plaque assays were carried out as described in "Materials and methods". **a** MDCK cells were infected with virus suspension (500 pfu/ml) and then overlaid with the overlay medium containing various concentrations of EGb. The profile of plaques is shown in the *right panels*. *Panels 1*, *2*, *3*, *4*, *5* and *6* represent assays carried out in the presence of 0, 0.625, 1.25, 2.5, 5 and 10 μg/ml of EGb, respectively. **b** Influenza A virus (500 pfu/ml) was incubated with various concentrations of EGb prior to exposure to MDCK cells. The profile of plaques is shown in the *right panels*. *Panels 1*, *2*, *3*, *4*, *5* and *6* represent assays in the presence of 0, 0.625, 1.25, 2.5, 5 and 10 μg/ml of EGb, respectively. Results are represented as the percentage of the plaque number formed in the absence of EGb

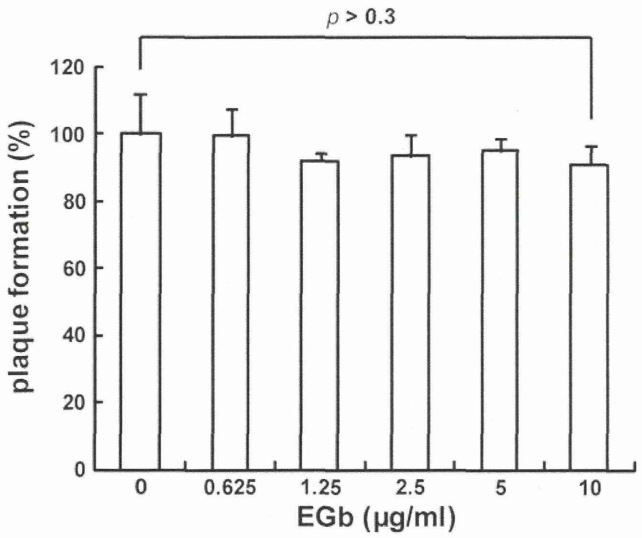

Fig. 3 Effect of pre-treatment of host cells with EGb on influenza virus infection. MDCK cells were exposed to EGb at various concentrations and incubated at 37 °C for 1 h prior to virus infections. After removing EGb, MDCK cells were inoculated with influenza A/PR/8/34 viruses (500 pfu/ml), and plaque formation assays were carried out as described in "Materials and methods". Results are represented as the percentage of the plaque number formed in the absence of EGb. All data are represented as mean ± SD, and the statistical analysis was performed using the *t* test to compare two groups

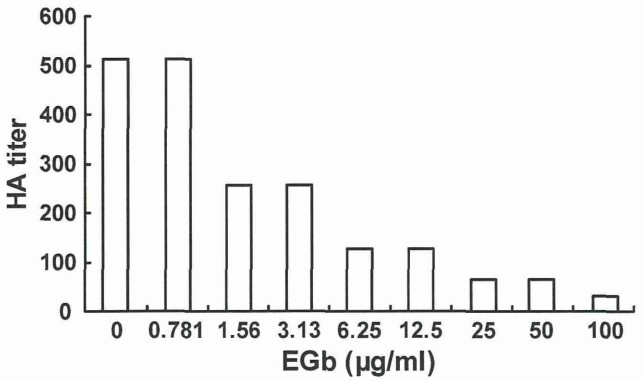

Fig. 4 HA titers of influenza A virus treated with various concentrations of EGb. Influenza A/PR/8/34 virus and EGb were diluted by twofold dilution each time and then mixed. After incubation at room temperature for 5 min, 0.5 % chicken erythrocyte suspension was added to each of these mixtures in a 96-well assay plate, and the plate was incubated at room temperature for 30 min for hemagglutination. Results are represented as a plot where the *x*-axis and *y*-axis indicate concentrations of EGb and HA titer, respectively. The result is representative of three independent experiments

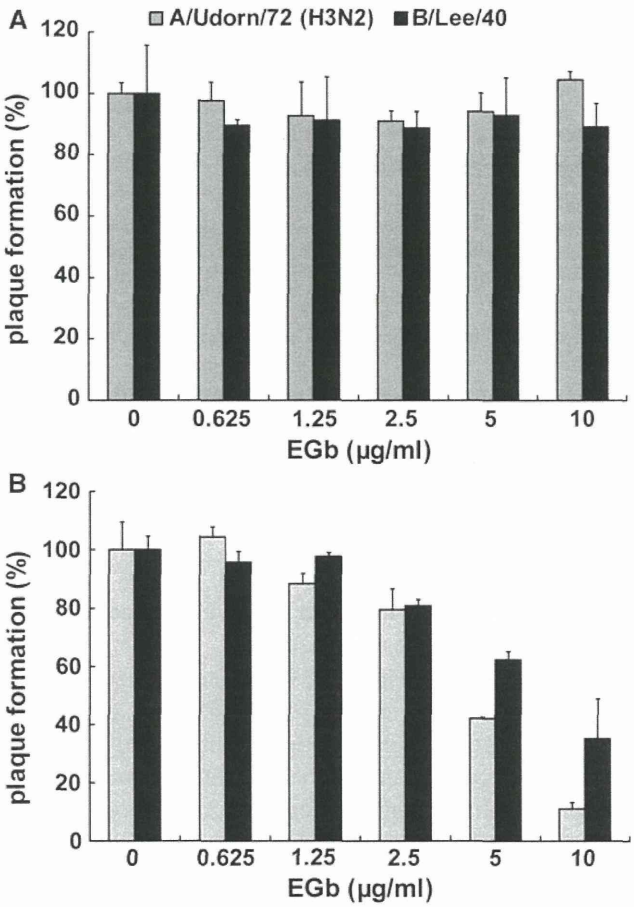

Fig. 5 Effect of EGb on plaque formation by two different subtypes of influenza virus. Plaque assays were carried out as described in "Materials and methods". **a** MDCK cells were infected with 0.5 ml of 500 pfu/ml of influenza A/Udorn/72 (H3N2) and B/Lee/40 viruses and then overlaid with the overlay medium containing various concentrations of EGb. **b** Each influenza virus strain was diluted to 500 pfu/ml and incubated with various concentrations of EGb prior to exposure to MDCK cells. One hour after virus inoculation, MDCK cells were washed with serum-free MEM and subsequently overlaid with the overlay medium without EGb. Results are represented as the percentage of the plaque number formed in the absence of EGb. **a**, **b** Results of A/Udorn/72 (H3N2) and B/Lee/40 are represented by *gray bars* and *black bars*, respectively

with slightly different sensitivities. To confirm the difference in infectivity inhibition, the 50 % inhibitory concentration (IC_{50}) value of EGb was calculated for these three different strains of influenza viruses. Furthermore, the selectivity index (SI) was also calculated as the ratio of CC_{50} to IC_{50} (Table 1). The influenza A/PR/8/34 virus showed most sensitivity to EGb (Table 1). These findings suggest that the antiviral activity of EGb is not dependent on the type of influenza virus.

Discussion

In this study, we revealed the anti-influenza virus activity of *Ginkgo biloba* leaf extract (EGb). EGb acted directly on the influenza viruses and prevented their adsorption to the host cell surface, suggesting that EGb interfered with the interaction between the HA on the influenza virion and sialic acids on the host cell surface, although we could not

Table 1 Selectivity indices of EGb in three different influenza virus strains

Virus strain	IC_{50} (μg/ml)[a]	SI[b]
A/PR/8/34 (H1N1)	1.86	96.8
A/Udorn/72 (H3N2)	4.41	40.8
B/Lee/40	6.79	26.5

[a] IC_{50}: 50 % inhibitory concentration of EGb was calculated from the results of the plaque formation assay performed as shown in Figs. 2b and 5b

[b] SI: selectivity index was evaluated as the ratio of CC_{50} to IC_{50}, i.e., $SI = CC_{50}/IC_{50}$

CC_{50}: 50 % cytotoxic concentration of EGb was calculated from the dose–response curve shown in Fig. 1a and its value (=180 μg/ml) was used for the calculation of each SI

All calculation was performed by using GraphPad Prism software as described in "Materials and methods"

exclude the possibility that EGb had a viricidal activity and directly inactivated the influenza virus.

The active constituents of EGb are standardized around the world; i.e., they contain 24 % flavonol glycosides (quercetin, kaempferol and isorhamnetin) and 6 % terpene lactones (ginkgolides and bilobalide). EGb also contains a class of condensed tannins, which are polymers composed primarily of flavan-3-ols (catechin and epicatechin) with a covalent bond between the individual flavonol units. Nakayama et al. [10] previously reported that two condensed tannins present in teas, (−)-epigallocatechin gallate (EGCG) and theaflavin digallate, bind to the HA of the influenza virus and inhibit its adsorption to MDCK cells. Furthermore, Song et al. [12] showed that catechin derivatives, including EGCG from green tea, inhibit not only the hemagglutination but also the NA activity of the influenza virus. The neuraminidase activity is thought to play a key role in the release of progeny virions from infected cells by cleavage of the sialic acid moieties of host cell receptors and in the prevention of self-aggregation of virions by cleavage of sialic acid still bound to the virus surface. These findings provide important insights into the molecular mechanisms of action of EGb.

Ginkgetin, a biflavone originally isolated from *Ginkgo biloba* leaves, has been found to inhibit the influenza virus sialidase [7]. However, our results showed that EGb prevented adsorption in the initial step of influenza virus infection. Therefore, in our study, a substance(s) in EGb other than ginkgetin may have been effective against influenza virus infection.

EGb was effective against the three different types of influenza viruses tested here, viz., the influenza A/PR/8/34 (H1N1), A/Udorn/72 (H3N2), and B/Lee/40 viruses, although the sensitivity towards EGb was slightly different among the three viruses. This finding suggests that EGb may be a potential wide-range inhibitor against influenza virus infection.

When plaque assays were performed with overlay medium containing EGb, neither the number of plaques nor their sizes were affected (Fig. 2a). Since our results suggest that EGb acts directly on the influenza virus and prevents the initial step in viral infection, we expected that the infectivity of the progenitor virions would be decreased owing to interaction with EGb present in the overlay medium and, consequently, that the size of individual plaques would be reduced in the plaque assay. This discrepancy between the predicted and the experimental results may be explained by our recent findings: we disclosed a novel transmission mode for influenza viruses, the so-called cell-to-cell transmission mode [8]. Influenza viruses have generally been believed to be capable of spreading via *cell-free* virions released from infected cells depending on the activity of NA. However, in cell-to-cell transmission, progeny virions are retained on the infected cell surface even after budding and transmitted from infected cells to adjacent uninfected cells without being released into the outer environment. The cell-to-cell transmission of the influenza virus is dependent on functional HA but independent of NA activity. The present study may demonstrate that EGb cannot inhibit the cell-to-cell transmission of influenza viruses but is highly effective in decreasing the infectivity of *cell-free* virions. This suggestion is in line with the findings of a previous study in which higher concentrations of anti-HA antibody were needed for inhibition of infection through cell-to-cell transmission than for that through *cell-free* viruses [8].

The plaque assay using drug-containing agarose gels is one of the most reliable methods for detecting anti-influenza virus activity and is frequently used as a screening method. However, our findings raise concerns that a particular anti-influenza virus activity, such as the inhibitory effect found here in EGb, may have been largely overlooked in past studies.

In conclusion, we have shown that EGb interacts directly with influenza viruses and markedly reduces the infectivity of the viruses by preventing their adsorption to host cells. Furthermore, the inhibitory effect of EGb seemed not to be restricted to a certain subtype of influenza virus. Taken together, these findings indicate the usefulness of EGb as an antiviral agent for influenza, although further studies are necessary to confirm its anti-influenza virus activity in vivo.

In addition to the finding of the anti-influenza virus activity of EGb, we demonstrated an interesting and important insight(s) into the screening system for anti-influenza virus activity. As was the case for the anti-influenza virus activity of EGb found in this study, some candidates for antiviral agents may have been overlooked

in past studies because of the existence of the cell-to-cell transmission mode of influenza viruses. Therefore, our results signal a need for caution on the part of investigators trying to find anti-influenza virus compounds.

Acknowledgments We thank Katsushi Ogami and Yasuyuki Oku (Mitsubishi Paper Mills Ltd.) and Dr. Eri Nobusawa (Nagoya City University) for providing us with EGb and influenza B/Lee/40 viruses, respectively. We also thank Flaminia Miyamasu (Medical English Communication Center of Faculty of Medicine) for proofreading of this manuscript. This work was supported in part by a Grant-in-Aid from the Ministry of Education, Culture, Sports, Science and Technology of Japan (KN) and a Grant for the project of Tsukuba Industrial Liaison and Cooperative Research (KN).

References

1. Chan PC, Xia Q, Fu PP (2007) *Ginkgo biloba* leave extract: biological, medicinal, and toxicological effects. J Environ Sci Health C Environ Carcinog Ecotoxicol Rev 25:211–244
2. DeFeudis FV, Drieu K (2000) *Ginkgo biloba* extract (EGb 761) and CNS functions: basic studies and clinical applications. Curr Drug Targets 1:25–58
3. Diamond BJ, Shiflett SC, Feiwel N, Matheis RJ, Noskin O, Richards JA, Schoenberger NE (2000) *Ginkgo biloba* extract: mechanisms and clinical indications. Arch Phys Med Rehabil 81:668–678
4. Drieu K (1986) Preparation and definition of *Ginkgo biloba* extract. Presse Med 15:1455–1457
5. Lichtblau D, Berger JM, Nakanishi K (2002) Efficient extraction of ginkgolides and bilobalide from *Ginkgo biloba* leaves. J Nat Prod 65:1501–1504
6. Long JK, Mossad SB, Goldman MP (2000) Antiviral agents for treating influenza. Cleve Clin J Med 67:92–95
7. Miki K, Nagai T, Suzuki K, Tsujimura R, Koyama K, Kinoshita K, Furuhata K, Yamada H, Takahashi K (2007) Anti-influenza virus activity of biflavonoids. Bioorg Med Chem Lett 17:772–775
8. Mori K, Haruyama T, Nagata K (2011) Tamiflu-resistant but HA-mediated cell-to-cell transmission through apical membranes of cell-associated influenza viruses. PLoS ONE 6(11):e28178
9. Nagata K, Sakagami H, Harada H, Nonoyama M, Ishihama A, Konno K (1990) Inhibition of influenza virus infection by pine cone antitumor substances. Antivir Res 13:11–21
10. Nakayama M, Suzuki K, Toda M, Okubo S, Hara Y, Shimamura T (1993) Inhibition of the infectivity of influenza virus by tea polyphenols. Antivir Res 21:289–299
11. Regoes RR, Bonhoeffer S (2006) Emergence of drug-resistant influenza virus: population dynamical considerations. Science 312:389–391
12. Song J, Lee K, Seong B (2005) Antiviral effect of catechins in green tea on influenza virus. Antivir Res 68:66–74
13. Turan K, Nagata K, Kuru A (1996) Antiviral effect of *Sanicula europaea* L. leaves extract on influenza virus-infected cells. Biochem Biophys Res Commun 225:22–26
14. Wang X, Jia W, Zhao A, Wang X (2006) Anti-influenza agents from plants and traditional Chinese medicine. Phytother Res 20:335–341
15. Watanabe K, Momose F, Handa H, Nagata K (1995) Interaction between influenza virus proteins and pine cone antitumor substance that inhibits the virus multiplication. Biochem Biophys Res Commun 214:318–323
16. Wiley DC, Skehel JJ (1987) The structure and function of the hemagglutinin membrane glycoprotein of influenza virus. Annu Rev Biochem 56:365–394
17. Yoshikawa T, Naito Y, Kondo M (1999) *Ginkgo biloba* leaf extract: review of biological actions and clinical applications. Antioxid Redox Signal 1:469–480

OPEN ACCESS Freely available online

PLOS ONE

Critical Role of an Antiviral Stress Granule Containing RIG-I and PKR in Viral Detection and Innate Immunity

Koji Onomoto[1,2,9¤], Michihiko Jogi[1,3,4], Ji-Seung Yoo[1,3], Ryo Narita[1], Shiho Morimoto[1], Azumi Takemura[1], Suryaprakash Sambhara[5], Atushi Kawaguchi[6,7], Suguru Osari[6], Kyosuke Nagata[6], Tomoh Matsumiya[8], Hideo Namiki[9], Mitsutoshi Yoneyama[4,10]*, Takashi Fujita[1,3]*

1 Laboratory of Molecular Genetics, Institute for Virus Research, Kyoto University, Kyoto, Japan, **2** Research Institute for Science and Engineering, Waseda University, Tokyo, Japan, **3** Laboratory of Molecular Cell Biology, Graduate School of Biostudies, Kyoto University, Kyoto, Japan, **4** Division of Molecular Immunology, Medical Mycology Research Center, Chiba University, Chuo-ku, Chiba, Japan, **5** Influenza Division, Centers for Disease Control and Prevention, Atlanta, Georgia, United States of America, **6** Department of Infection Biology, Faculty of Medicine and Graduate School of Comprehensive Human Sciences, University of Tsukuba, Tsukuba, Japan, **7** Kitasato Institute for Life Sciences, Kitasato University, Tokyo, Japan, **8** Department of Vascular Biology, Institute of Brain Science, Graduate School of Medicine, Hirosaki University, Aomori, Japan, **9** Graduate School of Science and Engineering, Waseda University, Tokyo, Japan, **10** PRESTO, Japan Science and Technology Agency, Honcho Kawaguchi, Saitama, Japan

Abstract

Retinoic acid inducible gene I (RIG-I)-like receptors (RLRs) function as cytoplasmic sensors for viral RNA to initiate antiviral responses including type I interferon (IFN) production. It has been unclear how RIG-I encounters and senses viral RNA. To address this issue, we examined intracellular localization of RIG-I in response to viral infection using newly generated anti-RIG-I antibody. Immunohistochemical analysis revealed that RLRs localized in virus-induced granules containing stress granule (SG) markers together with viral RNA and antiviral proteins. Because of similarity in morphology and components, we termed these aggregates antiviral stress granules (avSGs). Influenza A virus (IAV) deficient in non-structural protein 1 (NS1) efficiently generated avSGs as well as IFN, however IAV encoding NS1 produced little. Inhibition of avSGs formation by removal of either the SG component or double-stranded RNA (dsRNA)-dependent protein kinase (PKR) resulted in diminished IFN production and concomitant enhancement of viral replication. Furthermore, we observed that transfection of dsRNA resulted in IFN production in an avSGs-dependent manner. These results strongly suggest that the avSG is the locus for non-self RNA sensing and the orchestration of multiple proteins is critical in the triggering of antiviral responses.

Citation: Onomoto K, Jogi M, Yoo J-S, Narita R, Morimoto S, et al. (2012) Critical Role of an Antiviral Stress Granule Containing RIG-I and PKR in Viral Detection and Innate Immunity. PLoS ONE 7(8): e43031. doi:10.1371/journal.pone.0043031

Editor: Akio Kanai, Keio University, Japan

Received April 11, 2012; **Accepted** July 16, 2012; **Published** August 13, 2012

Funding: The Ministry of Education, Culture, Sports, Science and Technology in Japan (Innovative Areas "RNA regulation" (No.20112009), Scientific Research "A", and Research Activity Start-up) (http://www.mext.go.jp/english/), the Ministry of Health, Labour and Welfare of Japan (http://www.mhlw.go.jp/english/index.html), the PRESTO Japan Science and Technology Agency (http://www.jst.go.jp/kisoken/presto/index_e.html), the Uehara Memorial Foundation (http://www.ueharazaidan.com/), the Mochida Memorial Foundation for Medical and Pharmaceutical Research (http://www.mochida.co.jp/zaidan/), the Takaeda Science Foundation (http://www.takeda-sci.or.jp/index.html), the Naito Foundation (http://www.naito-f.or.jp/), and Nippon Boehringer Ingelheim (http://www.boehringer-ingelheim.co.jp/com/Home/index.jsp). The funders had no role in study design, data collection and analysis, decision to publish, or preparation of the manuscript.

Competing Interests: The authors have the following competing interests: This study was partly funded by Nippon Boehringer Ingelheim. There are no patents, products in development or marketed products to declare. This does not alter the authors' adherence to all the PLoS ONE policies on sharing data and materials, as detailed online in the guide for authors.

* E-mail: myoneyam@faculty.chiba-u.jp (MY); tfujita@virus.kyoto-u.ac.jp (TF)

¤ Current address: Division of Molecular Immunology, Medical Mycology Research Center, Chiba University, Chuo-ku, Chiba, Japan

Introduction

Type I and III interferons (IFNs) are cytokines with strong antiviral activity [1,2]. Upon the binding of IFNs with their cognate receptor complexes, an intracellular signal is activated resulting in the activation of transcription factors, IFN stimulated gene factor 3, heterotrimer of signal transducer and activator of transcription (STAT)1, STAT2, and IFN regulatory factor (IRF)-9, and STAT1 homodimer. These factors induce the activation of hundreds of interferon stimulated genes (ISGs). Some of the ISG products act as antiviral proteins and participate in the blockade of viral replication. The level of double-stranded (ds) RNA-dependent protein kinase (PKR) is enhanced by IFN treatment, however catalytic activity of PKR requires dsRNA. When IFN-treated cells are infected by virus, dsRNA, produced as a by-product of viral replication, activates PKR, and the activated PKR inactivates eukaryotic translation initiation factor (eIF) 2á by phosphorylation [3]. Another antiviral protein 2′–5′ oligoadenylate synthetase (OAS) is also induced to express by IFN. Catalytic activity of OAS requires dsRNA and virus infection activates OAS to produce 2′–5′ A. 2′–5′ A then activates cellular RNase L, and viral RNA is degraded [1]. Although, the "dsRNA-activated inhibition" model is widely accepted, IFN-treated and virus-infected cells do not necessarily undergo suicide, as conventional IFN bioassays have demonstrated IFN-induced survival of infected cells [4]. To explain these phenomena, it has been hypothesized that viral transcription/translation takes place in a specific subcellular compartment, thus the blocking of translation and the degradation

of RNA by these antiviral proteins little affect host metabolism. However, no one has yet demonstrated such a compartment.

IFNs are not normally produced at biologically significant levels. Most types of mammalian cells are capable of producing IFN upon viral infection. Viral replication is sensed by cytoplasmic non-self RNA sensors; RIG-I, melanoma differentiation-associated gene 5 (MDA5), and laboratory of genetics and physiology 2 (LGP2), which are collectively termed RLRs, to initiate the cascade of events leading to the activation of transcription factors, IRF-3/-7 and nuclear factor-êB (NF-êB), then the activation of IFN genes [5–9]. Thus, the primary function of the IFN system is to sense non-self RNA and to eradicate the invading RNA, which includes RNA derived from the replication of DNA viruses [10,11]. Although genetic evidence shows that RLR is critical for detecting viral RNA in the cytoplasm, its specific distribution has been unknown.

In this report, we investigated the cellular localization of RIG-I in Influenza A Virus -infected cells. We discovered that viral infection or the transfection of viral RNA causes RIG-I to form granular aggregates containing stress granule markers, which we term antiviral stress granules (avSGs). Our analyses revealed that avSGs are critical for signaling to activate the IFN gene, suggesting that the avSG serves as a platform for the sensing of non-self RNA by RLRs. Furthermore, because the granule also recruits PKR, OAS and RNase L, it is strongly suggested to be the compartment where some antiviral proteins inhibit viral replication.

Results

Infection of NS1-deficient IAV Produces Granules Containing RIG-I

We generated an anti-RIG-I antibody, which specifically detects RIG-I by immunostaining and immunoblotting (Figure S1) (Materials and Methods) [12]. To observe the cellular distribution of RIG-I, cells were infected with two types of IAV, the wild type (WT) and ÄNS1 which lacks the gene for non-structural protein 1 (NS1), a potent inhibitor of IFN production [13]. WT IAV replication was detectable at 3 h after infection as a nuclear accumulation of viral nucleocapsid protein (NP) (Figure 1A). Later in the infection (9–12 h), NP, presumably as a complex with viral genomic RNA [14], translocated to the cytoplasm. RIG-I was dispersed in uninfected cells and WT IAV infection did not cause any change in its distribution. On the other hand, in cells infected with IAVÄNS1, NP accumulated in the nucleus at 6 h post-infection, however only a fraction of NP translocated to the cytoplasm at 9–12 h (Figure 1B). Unlike WT IAV, the NP of IAVÄNS1 exhibited a speckle-like distribution in the cytoplasm. Notably, formation of this RIG-I-containing speckle strongly correlates with activation of RIG-I-mediated signal activation as judged by nuclear localization (Figure 1C) and dimerization of IRF-3 and concomitant enhanced production of ISGs, such as RLRs and STAT1 (Data not shown). Indeed, the ratio of cells with IAV- and IAVÄNS1-induced nuclear IRF-3 was 2.7% and 33.7%, respectively, and cells containing RIG-I speckles together with nuclear IRF-3 were 0.0% (IAV) and 72.2% (IAVÄNS1).

IAVÄNS1-induced Granules Contain Both Stress Granule Marker and Anti-viral Proteins

We characterized the nature of these speckles by using various antibodies and found that interestingly, RIG-I exhibited co-localization with NP (83.5%) and a stress granule (SG) marker, T-cell restricted intracellular antigen-related protein (TIAR) (97.1%) at 9 h (Figure 1B). Other SG markers are similarly recruited to the granules produced by IAVÄNS1: Ras-GAP SH3 domain-binding protein (G3BP) (97.6% colocalized with RIG-I), eIF3 (99.8% colocalized with G3BP) (Figure 1D and 1E), and human antigen R (HuR) (98.8% colocalized with RIG-I) (data not shown). Furthermore, physical interaction between RIG-I and SG markers was demonstrated by pull-down assays (Figure 1F). These results strongly suggest that although IAV infection potentially induces signaling to activate the IFN gene and the formation of granular aggregates containing SG markers, NS1 strongly blocks both. Ectopic expression of full-length NS1 and the N-terminal RNA-binding domain of NS1 dramatically inhibited both granule-formation and RIG-I signaling in response to IAVÄNS1 infection, indicating that the N-terminal domain of NS1 is responsible for these activities (Figure S2A and S2B).

SGs are an intracellular ribonucleoprotein (RNP) complex generated by cellular stress, including oxidative, heat shock, and endoplasmic reticulum stress, and contain translation-stalled mRNAs and various RNA-binding proteins [15]. Because many of the SG markers are RNA-binding proteins, we examined the localization of other RLRs, MDA5, and LGP2, as well as PKR (see below), RNase L, and OAS by using specific antibodies. Interestingly, these proteins were also recruited to SG and virus-induced granules in response to arsenite and IAVÄNS1, respectively (Figure 2A, 2B, 2C, 2D).

IAVÄNS1 Infection Induces Antiviral SGs Containing Viral RNA

These results prompted us to examine correlation between the formation of SGs and activation of the IFN gene. Treatment of cells with arsenite ($NaAsO_2$), which induced oxidative stress, produced granules similar to those generated by IAVÄNS1 (Figure 3A). Similarly, artificial overexpression of PKR resulted in the formation of SGs (58.9%) (Figure 3A). Although IAVÄNS1 infection activated the IFN-â gene, neither arsenite nor PKR activated the gene (Figure 3B). These results suggest that SGs and virus-induced granules are functionally distinct, possibly due to the presence of viral RNA in virus-induced granules. Indeed, fluorescence *in situ* hybridization (FISH) clearly demonstrated that viral RNA colocalized with the granules of NP (Figure 3C) and RIG-I (Figure 3D) in IAVÄNS1-infected cells whereas IAV-infected cells showed colocalization of viral RNA with NP (Figure S3A) but not with RIG-I (Figure S3B). Once viral RNA is engaged by RIG-I-containing complex, IFN-â promoter stimulator-1 (IPS-1, also known as MAVS, VISA or Cardif) expressed on the outer membrane of mitochondria is recruited to facilitate RIG-I-IPS1 signaling in a Mitofusin 1-dependent manner [12,16]. Although most of IPS-1 localizes on mitochondrial network in uninfected and IAV-infected cells, IAVÄNS1 infection induces speckle-like distribution. The re-localized IPS-1 exhibits apparent contacts with TIAR- (Figure 3E, bottom-right panel), and RIG-I- (Figure S4) containing SGs. This is consistent with a model that SG physically contacts with mitochondrion mediated by interaction between RIG-I and IPS-1 through caspase recruitment domain (CARD)-CARD homotypic interaction [17–20]. Although association of FLAG-tagged IPS-1 with peroxisome membrane protein (PMP70)-positive peroxisomes after viral infection was reported [21], we did not observe their apparent association (Figure 3E).

SG production is not a result of RIG-I signaling or IFN signaling because overexpression of IPS-1 activated the nuclear translocation of IRF-3 without generating SGs (Figure S5A), and SGs formed in IFN receptor-deficient HEC-1B cells (Figure S5B). Furthermore, other viruses including Sindbis (SINV), encephalomyocarditis (EMCV), and Adeno (Ad) dl203 viruses also generated granules containing RIG-I and G3BP (Figure S5C), suggesting this SG-like granule to be a general response to viral infections. To

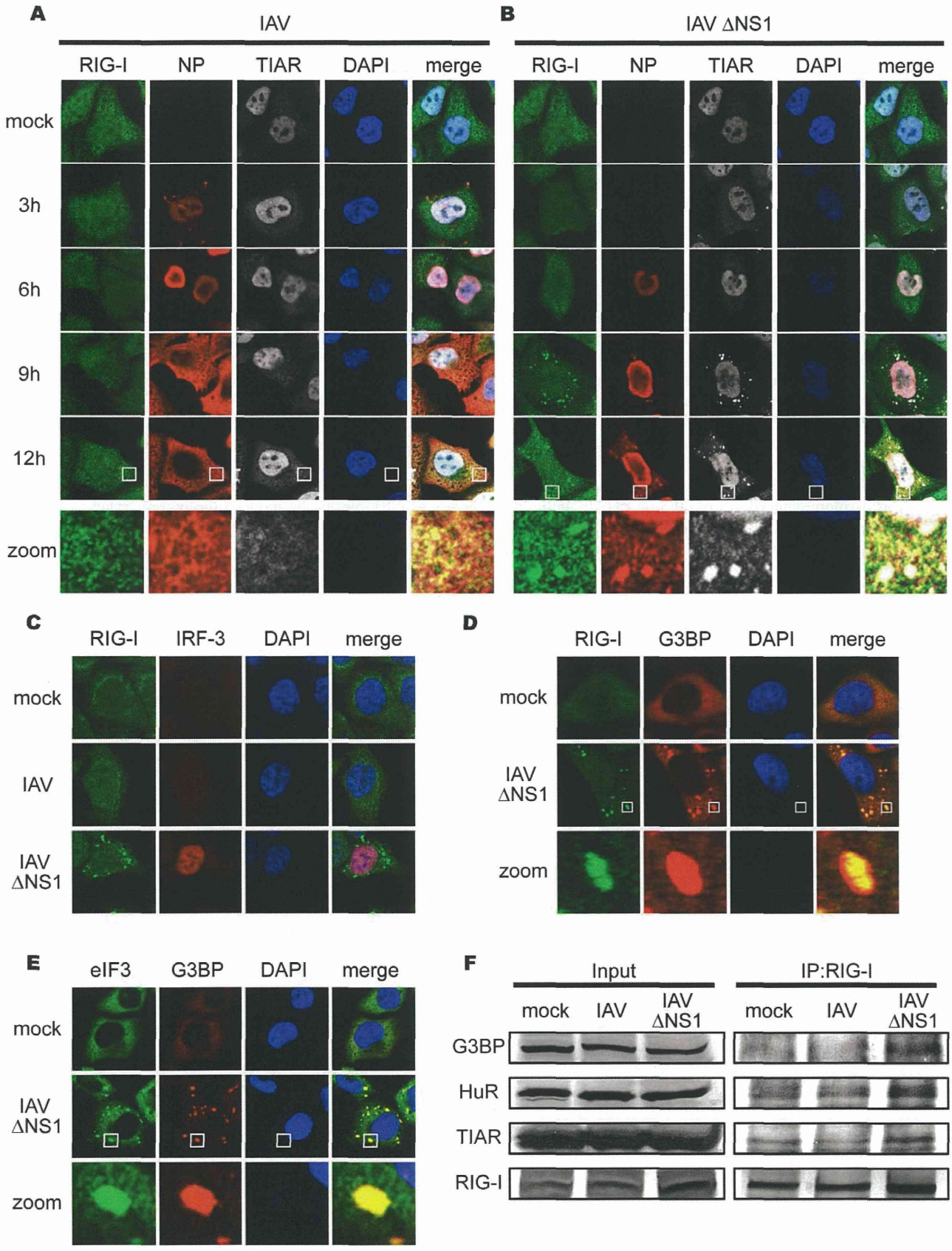

Figure 1. IAV infection causes a speckle-like distribution of RIG-I and stress granule markers. (**A–C**) HeLa cells were mock-treated or infected with IAV (**A**) or IAVÄNS1 (**B**) for the indicated period, fixed, stained, and analyzed with confocal microscopy. The cells were stained with anti-RIG-I (RIG-I), anti-IAV nucleocapsid protein (NP), and anti-TIAR (TIAR) antibodies. Nuclei were stained with DAPI. At 9 h and 12 h after infection, the

percentage of speckle-like distribution of RIG-I was 0.5% and 0.0% in IAV-infected cells, and 62.4% and 83.6% in IAVÄNS1-infected cells, respectively. The zoomed images correspond to the boxed region in each panel. The cells at 9 h post infection were stained with anti-RIG-I and anti-IRF-3 antibodies (**C**). (**D and E**) HeLa cells were infected with IAVÄNS1 for 9 h, and stained with anti-G3BP (G3BP), together with anti-RIG-I (RIG-I) (**D**) or anti-eIF3 (eIF3) (**E**). The zoomed images correspond to the boxed regions. (**F**) HeLa cells were mock-treated or infected with IAV or IAVÄNS1 for 12 h. Cell extracts were prepared and immunoprecipitated with anti-RIG-I antibody. The precipitates were analyzed by immunoblotting (IP:RIG-I) using antibody against G3BP, HuR, TIAR and RIG-I. Input: 1/50 of the extracts used for immunoprecipitation were analyzed similarly by immunoblotting.
doi:10.1371/journal.pone.0043031.g001

distinguish virus-induced granules from conventional SGs, we termed the virus-induced speckles as antiviral SGs (avSGs).

Impairment of Formation of avSGs Inhibits IAVÄNS1-induced IFN Activation

In order to address whether the formation of avSGs is required for IFN expression, we knocked down G3BP, a critical component for formation of the canonical SGs. G3BP siRNA clearly down-regulated G3BP expression (Figure 4A). Consistent with a previous study [22], the knockdown of G3BP strongly inhibited avSG formation in IAVÄNS1-infected cells (Figure 4B), and the number of cells which showed a speckle-like distribution of RIG-I and TIAR was diminished (Figure 4C and 4D). Moreover, IFN-â gene expression was strongly inhibited in G3BP knockdown cells compared to control siRNA-treated cells (Figure 4E). These results suggest that avSG formation is required for efficient activation of type I IFN. Furthermore, knockdown of eIF3 or RHAU, both of which are components of SG, also blocked both avSG formation and IFN gene activation (data not shown).

IAVÄNS1 Infection Induces PKR's Activation and Accumulation in avSGs

It has been proposed that a family of protein kinases including PKR, general control non-derepressible 2 (GCN2), PKR-like endoplasmic reticulum kinase (PERK), and heme-regulated eIF2á kinase (HRI) phosphorylate eIF2á, resulting in formation of SGs. Arsenite treatment causes oxidative stress leading to the activation of HRI, and SGs are produced. PKR is activated by dsRNA or 5¢ppp-containing RNA [23], therefore we speculate that the IAV RNA activates PKR resulting in the formation of avSGs via the phosphorylation of eIF2á. To address the involvement of PKR, we examined the localization of PKR in arsenite-treated and IAVÄNS1-infected cells and found that PKR accumulated in SGs and avSGs (Figure 5A). Interestingly, phosphorylated eIF2á was also detected in avSGs specifically generated by IAVÄNS1 but not in IAV-infected cells (Figure 5B). Immunoblotting confirmed that IAVÄNS1 specifically induced the phosphorylation of PKR and eIF2á whereas arsenite treatment induced the phosphorylation of eIF2á without PKR activation, indicating that IAVÄNS1 and arsenite induce SGs via distinct pathways (Figure 5C).

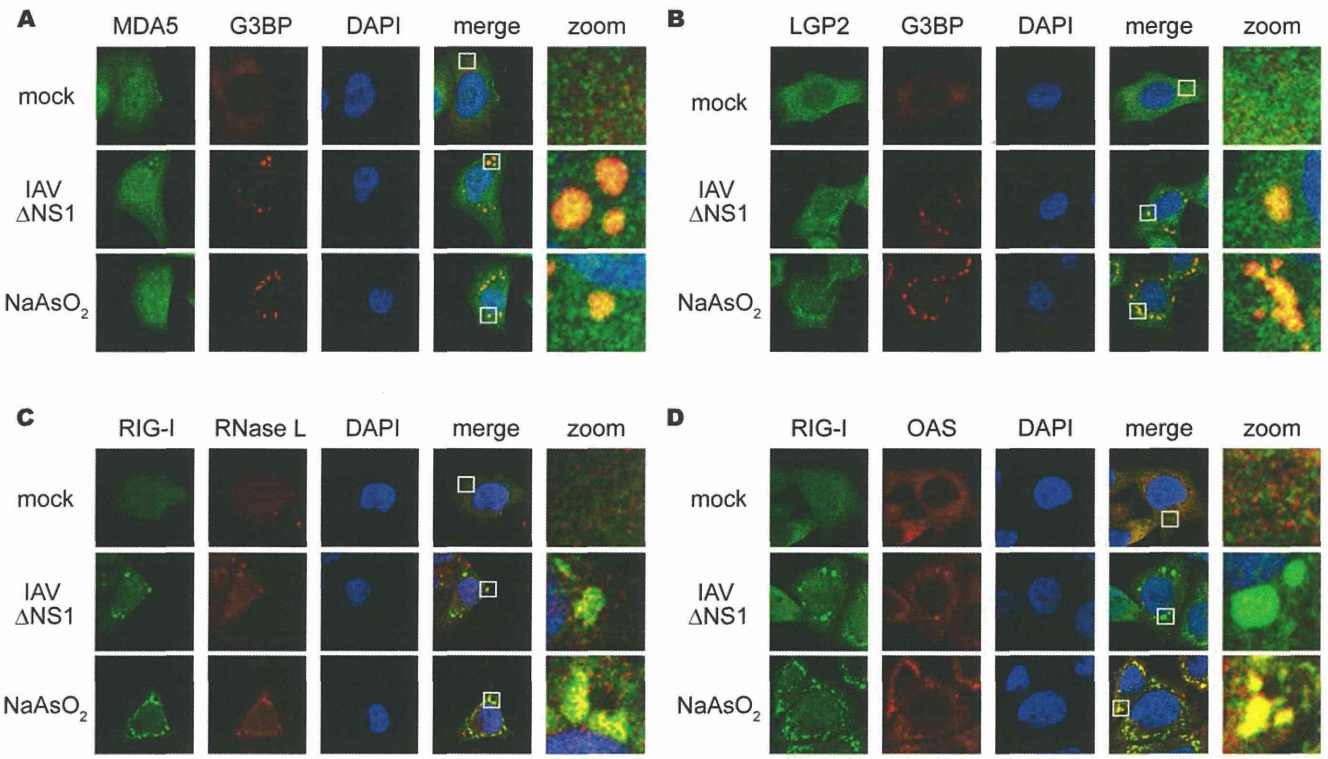

Figure 2. Antiviral proteins are colocalized with SGs. (**A–D**) HeLa cells were mock-treated (mock), infected with IAVÄNS1 for 9 h, or treated with $NaAsO_2$ for 1 h. Cells were fixed and stained for G3BP and MDA5 (94.2% colocalization) (**A**), G3BP and LGP2 (97.6% colocalization) (**B**), RIG-I and RNase L (84.5% colocalization) (**C**), RIG-I and OAS (87.4% colocalization) (**D**) in IAVÄNS1-infected cells. The zoomed images correspond to the boxed regions.
doi:10.1371/journal.pone.0043031.g002

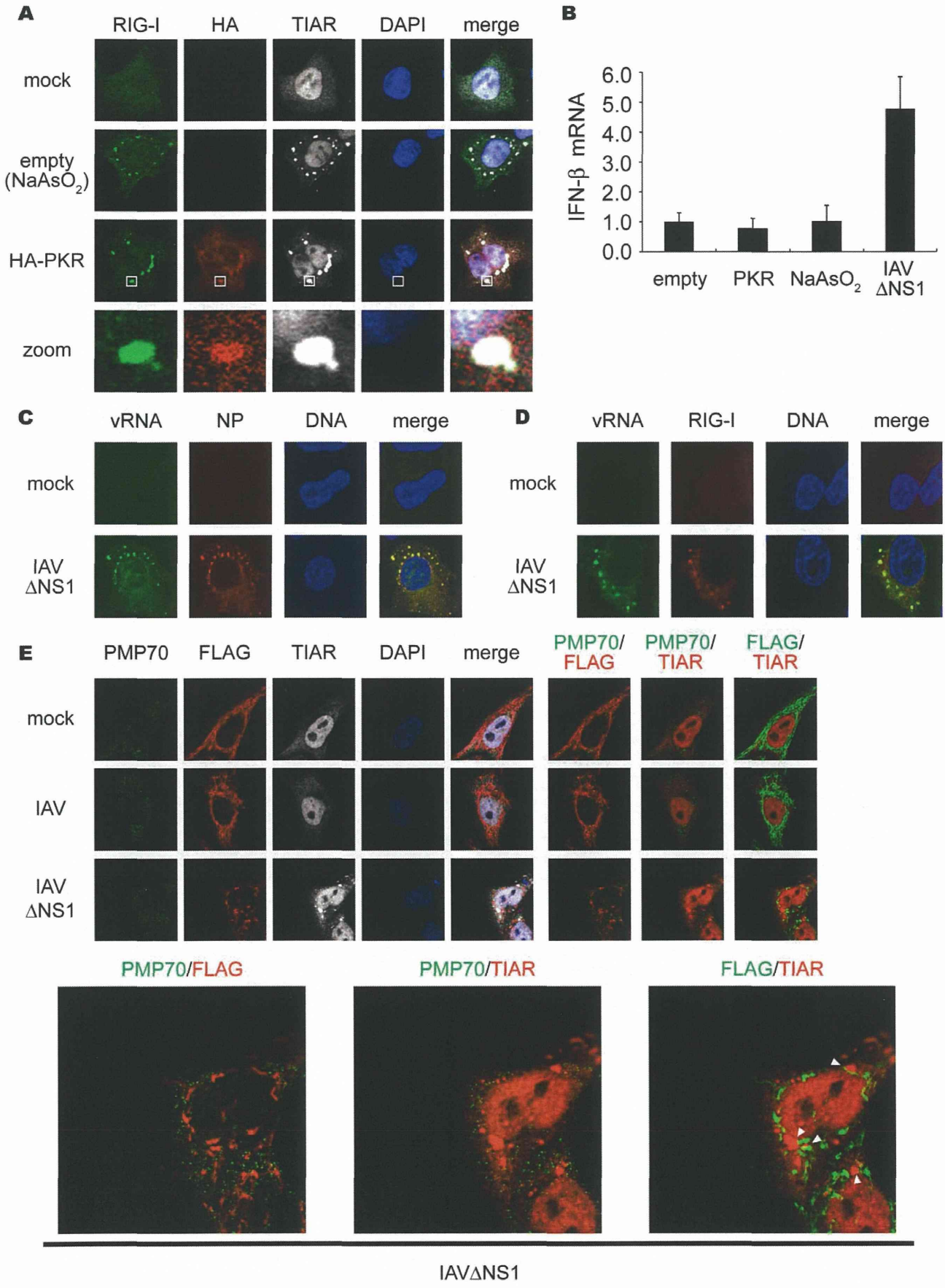
A
RIG-I
HA
TIAR
DAPI
merge
mock
empty (NaAsO2)
HA-PKR
zoom
B
IFN-β mRNA
6.0
5.0
4.0
3.0
2.0
1.0
0.0
empty
PKR
NaAsO2
IAV ΔNS1
C
vRNA
NP
DNA
merge
mock
IAV ΔNS1
D
vRNA
RIG-I
DNA
merge
mock
IAV ΔNS1
E
PMP70
FLAG
TIAR
DAPI
merge
PMP70/ FLAG
PMP70/ TIAR
FLAG/ TIAR
mock
IAV
IAV ΔNS1
PMP70/FLAG
PMP70/TIAR
FLAG/TIAR
IAVΔNS1

Figure 3. Viral RNA is required for formation of functional SG to activate RIG-I/IPS-1 signaling pathway. (**A**) 293T cells were transfected with empty vector (empty) or the HA-PKR expression vector (HA-PKR) for 24 h, or treated with $NaAsO_2$ for 1 h and stained with anti-RIG-I, anti-HA (PKR) and anti-TIAR antibodies and DAPI. The zoomed images correspond to the boxed regions. (**B**) 293T cells were transfected with empty vector (empty), or the HA-PKR expression vector for 48 h, or treated with $NaAsO_2$ for 1 h, or infected with IAVÄNS1 for 12 h. Relative mRNA levels of endogenous IFN-â gene were determined by quantitative PCR (qPCR). Data are represented as the mean standard ± error of the mean (SEM). (**C and D**) HeLa cells were mock-treated or infected with IAVÄNS1 for 12 h. Viral RNA (vRNA) was detected by the FISH method using an RNA probe complementary to the segment 1 of the IAV, and NP (**C**) and RIG-I (**D**) were detected using anti-NP and anti-RIG-I antibodies (97.1%, and 98.2% colocalization of vRNA with NP and RIG-I, respectively). TO-PRO-3 was used for staining of nuclear DNA (DNA). (**E**) HeLa cell lines stably expressing FLAG-tagged IPS-1 were mock-treated or infected with IAV or IAVÄNS1 for 10 h. The cells were stained with anti-PMP70, anti-FLAG, and anti-TIAR antibodies. The white arrowheads indicated the contacts between FLAG-IPS-1 and TIAR. 67.8% of IAVÄNS1 infected cells exhibited contacts, whereas IAV infected cells hardly exhibited the contact (2.7%). The zoomed images of PMP70 (Green) and FLAG (Red), PMP70 (Green) and TIAR (Red), and FLAG (Green) and TIAR (Red) in IAVÄNS1-infected cells were shown in the bottom panel.
doi:10.1371/journal.pone.0043031.g003

Critical Role of PKR in avSG Formation and IFN Production in IAV-infected Cells

The results described above indicate the formation of viral RNA-containing avSGs to be essential to RLR-mediated antiviral signaling. To evaluate the requirement of PKR during IAVÄNS1 infection, we analyzed the formation of avSGs in mouse embryonic fibroblasts (MEFs) derived from WT and PKR knock-out (KO) mice (Figure 6). PKR WT and KO MEFs were infected with either IAV or IAVÄNS1, and stained with the anti-RIG-I, anti-NP, and anti-TIAR antibodies and calculated the frequency of avSGs. In the case of WT IAV, avSGs did not form in WT and KO MEFs as determined in Figure 1. IAVÄNS1 produced avSGs in WT but not in PKR KO MEFs (Figure 6A, 6B, 6C). Moreover, deletion of PKR resulted in a blockade of IFN-â gene expression (Figure 6D), production of IFN-â protein (Figure 6E), and IRF-3 dimerization (Figure 6F). Furthermore, we confirmed these results using siRNA targeting PKR expression in HeLa cells. The siRNA efficiently knocked down endogenous

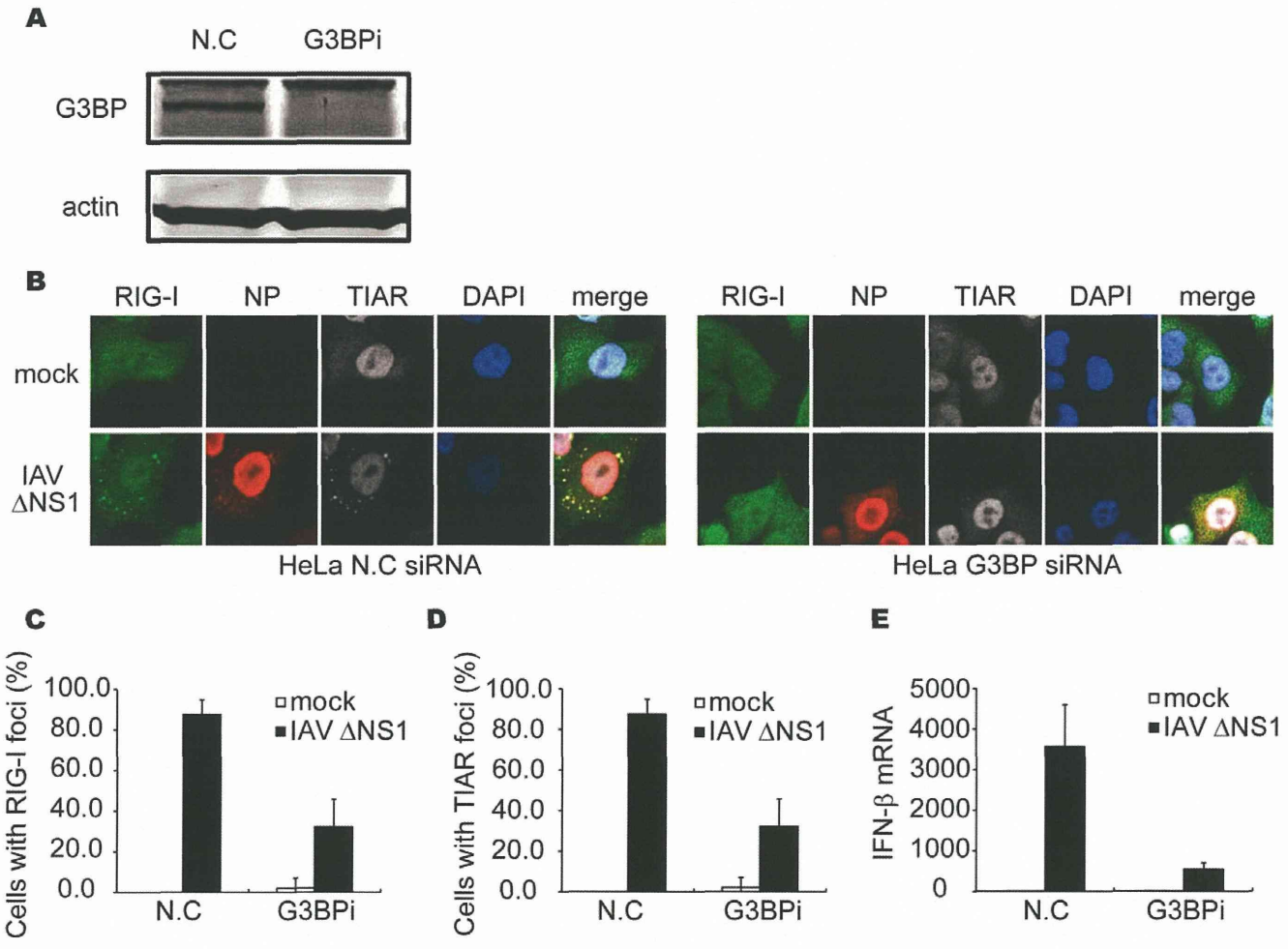

Figure 4. Knockdown of G3BP impairs formation of avSG and IFN-â gene activation. (**A–E**) HeLa cells were transfected with control siRNA (N.C) or siRNA targeting human G3BP (G3BPi). At 48 h after transfection, cells were harvested and G3BP and actin were detected by immunoblotting (**A**). Cells were mock-treated (mock) or infected with IAVÄNS1 for 12 h and fixed and stained with anti-RIG-I, anti-NP and anti-TIAR antibodies and DAPI (**B**). The percentage of cells containing foci of RIG-I (**C**) or TIAR (**D**) was determined. Relative mRNA level of IFN-â was determined by qPCR (**E**). Data are represented as the mean standard ± error of the mean (SEM).
doi:10.1371/journal.pone.0043031.g004